Jose et al., http://www.jcb.org/cgi/content/full/jcb.201206081/DC1

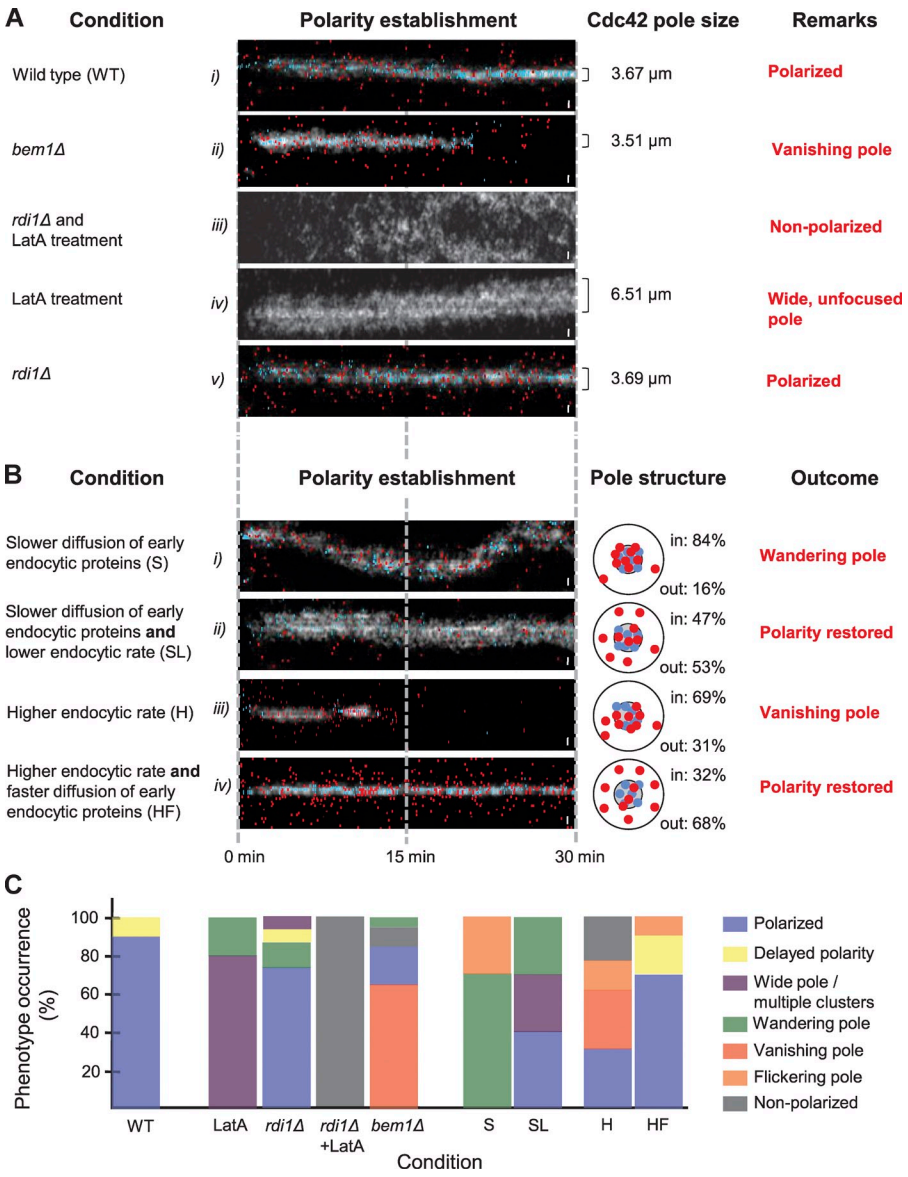

Figure S1. **Stable polarity requires both autoamplification and the segregation of endo- and exocytic events.** Transition of in silico cells under various conditions from nonpolarized (left) to a polarized state (right; time = 30 min). Kymographs show simulated membrane-bound Cdc42-GTP (grayscale) and individual endo- (red) and exocytic (cyan) events over time (x axis) along the cortex (y axis). Bars, 2 µm. (A) Autoamplification and Cdc42 recycling is required for stable polarity. In contrast to simulated WT cells displaying a stable, tight pole (*i*), in silico *bem1Δ* cells (*ii*, with reduced autoamplification) display Cdc42-GTP/GEF clusters that vanish within 10–20 min. This prediction is in agreement with the short-lived GEF clusters observed in *bem1Δ* cells in vivo, though some persistent Cdc42 clusters have also been reported in these mutants (Butty et al., 2002; Wedlich-Soldner et al., 2004). When both actin-dependent and -independent Cdc42 recycling pathways are disabled in the simulations, polarity is completely disrupted (*iii*). Simulations in which actin-dependent vesicle trafficking is disrupted show wide, stable Cdc42-GTP clusters (*iv*). In silico *rdi1Δ* cells, in which Cdc42-GDP cycling between membrane and cytosol is down-regulated, remained polarized (*v*). Results displayed in (*iii*–*v*) were in agreement with previous studies (Marco et al., 2007; Slaughter et al., 2009). The mean of the lateral extension of the Cdc42-GTP pole was calculated over 10 to 15 simulations. (B) Spatial segregation of endo- and exocytic events is required for stable polarity. Cells where endocytic events are triggered within the exocytic/Cdc42-GTP pole have been generated in silico, either by slowing down diffusion of early endocytic proteins from the pole ($D = 0.0025\ \mu m^2 s^{-1}$; *i*) or by increasing the frequency of endocytic events ($K_{en} = 3.34\ s^{-1}$; *iii*). In both cases, polarity was disrupted and could be restored by either decreasing the frequency of endocytic events to $K_{en} = 0.44\ s^{-1}$ in cells where the diffusion of early endocytic proteins is slow (*ii*) or by increasing the diffusion of endocytic proteins to $D = 0.144\ \mu m^2 s^{-1}$ in cells with high endocytic rates (*iv*). Polarized in silico cells with a high endocytic activity (*iv*) showed a tight Cdc42-GTP pole, contrary to cells having lower endocytic rates (*ii*), emphasizing the requirement for endocytosis in focusing the pole. Schematics show the typical distribution of endo- (red) and exocytic (cyan) events relative to the Cdc42-GTP pole (gray), and indicate the percentage of endocytic events happening "inside" and "outside" the pole. They show that polarity restoration correlates with spatial segregation of endo- and exocytic events. (C) Statistics of the different phenotypes predicted in silico under the conditions listed in A and B: normal polarity (A, *i*), vanishing pole (A, *ii*), absence of polarity (A, *iii*), wide pole (A, *iv*), and flickering and wandering pole (B, *i*). Statistics were obtained using 10 to 15 simulations.

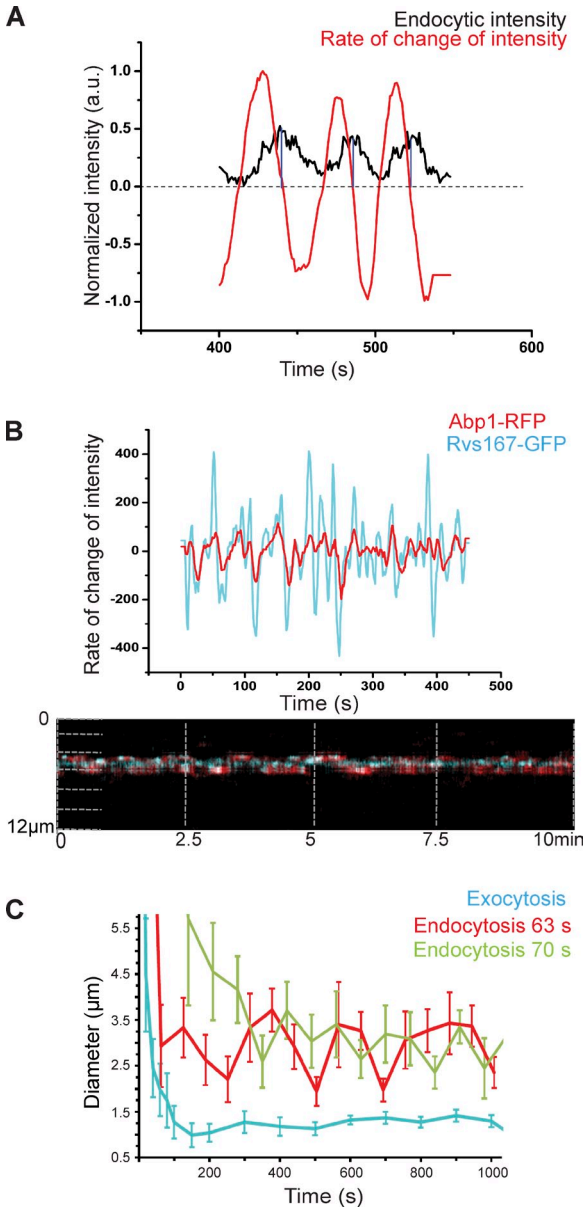

Figure S2. **Differentiating Abp1-RFP intensity fluctuations to monitor individual endocytic events and a graph showing that endocytic pole size is independent of the signal averaging time.** (A) The rate of change of intensity (dI/dt; red) shows the temporal change in the intensity distribution of each endocytic event (black) by a sine wave. dI/dt reaches maxima when the slope of the endocytic intensity starts to rise (black) and dI/dt tends to zero as the endocytic intensity reaches the peak (blue vertical line). The time interval between consecutive endocytic events is preserved after differentiation and smoothing. (B) Kymograph of a polarizing WT cell expressing Abp1-RFP (red) and Rvs167-GFP (cyan). The peaks in Abp1-RFP signal intensity (red) coincided with peaks in Rvs167-GFP intensity (cyan), a marker of endocytic vesicle scission, confirming that individual endocytic events were being monitored by Abp1-RFP. (C) The evolution of the endocytic pole size in silico does not show a strong dependence on the signal averaging time (M&M). The pole size is similar when calculated using an averaging time of 63 (red) or 70 s (green). Error bars and exocytic pole size (cyan) are defined as in Fig. 1 C.

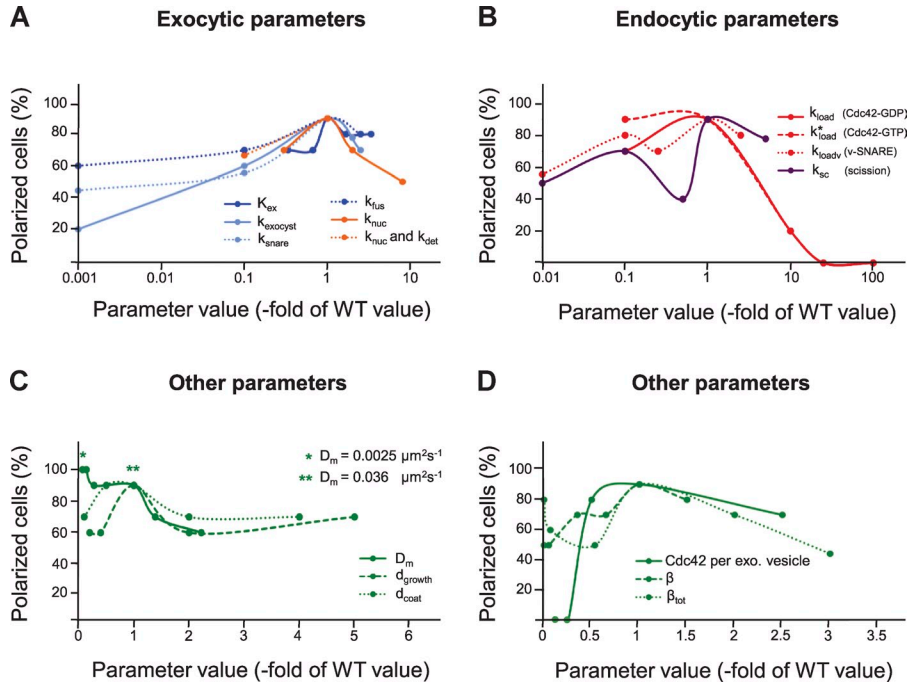

Figure S3. **Robustness of the multistability-based polarization mechanism to changes in parameters.** The vertical axis shows the percentage of polarized cells including delayed/wide polarity (each data point shows statistics in n = 10–15 simulations) when individual parameter values (horizontal axis) are modified. For each parameter, values are given in units of the WT value (see Table 1). Panels show that polarity is significantly affected by parameter changes only if Cdc42 has a very high affinity for endocytic vesicles (B, high values of k_{load} and k^*_{load}) or a very low affinity for exocytic vesicles (D).

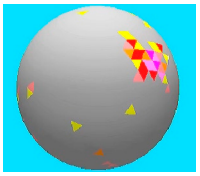

Video 1. **During polarity establishment in in silico WT cells, active Cdc42 is focused to a small region on the plasma membrane.** The movie shows a 20-min simulation of a polarizing WT cell in silico with Cdc42-GTP concentration shown as a heat map, from gray (low) to purple (high). Movie frames were exported individually from the Surface Evolver. The movie was played using the Evmovie software, and then converted to .mov format using screen capture under VirtualDub followed by h.264 compression in QuickTime.

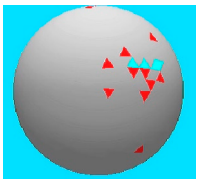

Video 2. **The reorganization of trafficking domains during polarity establishment in in silico WT cells.** The data shown originates from the same 20-min simulation used for Video 1 and depicts the polarization of endocytic events (red) corralling a tight zone of exocytosis (cyan). Movie frames were exported individually from the Surface Evolver. The movie was played using the Evmovie software, and then converted to .mov format using screen capture under VirtualDub followed by h.264 compression in QuickTime.

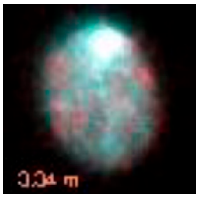

Video 3. **A polarizing WT cell in vivo displaying endocytic corralling of the exocytic zone.** GFP-Sec4 and Abp1-RFP are the exo- and endocytic markers, respectively. Images were acquired by dual-color video microscopy using a wide-field inverted microscope (Axiovert 200; Carl Zeiss). Frames were taken every second for 20 min. A median filter with a filter size of 3 × 3 was applied to the images for signal averaging before the making of the movie as an avi file. The time stamps for the movie were added in ImageJ.

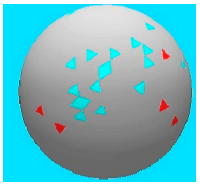

Video 4. **A *sla2Δ* cell in silico showing perturbed endocytic corralling.** The data shows 20 min of simulation in an in silico *sla2Δ* cell. Exocytic events (cyan) tend to cluster, but endocytosis (red) is spread over the membrane and exocytic clusters are unstable over time. Movie frames were exported individually from the Surface Evolver. The movie was played using the Evmovie software, and then converted to .mov format using screen capture under VirtualDub followed by h.264 compression in QuickTime.

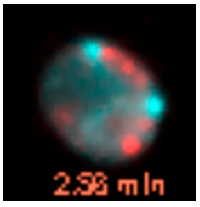

Video 5. **A polarizing *sla2Δ* cell in vivo showing perturbed endocytic corralling and multiple exocytic poles.** GFP-Sec4 and Abp1-RFP are the exo- and endocytic markers, respectively. Images were acquired by dual-color video microscopy using a wide-field inverted microscope. Frames were taken every second for 20 min. A median filter with a filter size of 3 × 3 was applied to the images for signal averaging before the making of the movie as an avi file. The time stamps for the movie were added in ImageJ.

References

Butty, A.C., N. Perrinjaquet, A. Petit, M. Jaquenoud, J.E. Segall, K. Hofmann, C. Zwahlen, and M. Peter. 2002. A positive feedback loop stabilizes the guanine-nucleotide exchange factor Cdc24 at sites of polarization. *EMBO J.* 21:1565–1576. http://dx.doi.org/10.1093/emboj/21.7.1565

Wedlich-Soldner, R., S.C. Wai, T. Schmidt, and R. Li. 2004. Robust cell polarity is a dynamic state established by coupling transport and GTPase signaling. *J. Cell Biol.* 166:889–900. http://dx.doi.org/10.1083/jcb.200405061

Marco, E., R. Wedlich-Soldner, R. Li, S.J. Altschuler, and L.F. Wu. 2007. Endocytosis optimizes the dynamic localization of membrane proteins that regulate cortical polarity. *Cell*. 129:411–422. http://dx.doi.org/10.1016/j.cell.2007.02.043

Slaughter, B.D., A. Das, J.W. Schwartz, B. Rubinstein, and R. Li. 2009. Dual modes of cdc42 recycling fine-tune polarized morphogenesis. *Dev. Cell*. 17:823–835. http://dx.doi.org/10.1016/j.devcel.2009.10.022

Provided online is a Matlab script calculating the concentration of Cdc42-GTP that solves the steady-state equations of the autoamplification module. The stability of the solutions is also tested.